Available online at www.sciencedirect.com
ScienceDirect
Ceramics International 38S (2012) S447–S451
CERAMICS INTERNATIONAL
www.elsevier.com/locate/ceramint

Unidirectional bulk conduction under trap density gradient for description of resistance switching

Yukio Watanabe *

Department of Physics, Kyushu University, Fukuoka, Fukuoka 812-8581, Japan

Available online 14 May 2011

Abstract

We show theoretically that under graded distributions of carrier traps nonlinear drift conduction exhibits diode-like characteristics, whereas at low voltage it exhibits ohmic characteristics that are symmetric with respect to the bias polarity. In shallow-trap dominated cases, the *JV* relationship of these diode-like characteristics is $J \propto V^m$ (J: current, V: voltage, $1 \leq m \leq 2$). These characteristics agree well with experiments. The theory reproduces exactly experimental *JV* characteristics using three free parameters in practice, only one more than that used in standard space charge-limited conduction theories. The results indicate that bulk-limited conduction can exhibit rectifying *JV* characteristics without relying on surface barriers. In most cases, the coexistence of deep traps with shallow-traps is necessary for the appearance of rectification.

Keywords: C. Electrical conductivity; C. Electrical properties; Diode; Resistance switching

1. Introduction

The conduction of various thin films, including those exhibiting resistance switching (*R*-switching), is conventionally discussed based on the surface-limited processes such as Schottky conduction. This is an appropriate approach because these thin films are thin and the bulk part of the thin films is of low resistance due to dislocations and defects. On the other hand, one may consider an opposite ideal limit: thick low-free-carrier-density material virtually without defects and dislocations. In this case, the conduction characteristics have been believed to be bidirectional. Indeed, the bidirectionality and unidirectionality of the conduction characteristics have been the clue for identifying the bulk- and surface-limited conduction.

In the thick low-free-carrier-density limit in the dark, the main conduction mechanism should be space-charge-limited (SCL) conduction [1]. Here, SCL theories incorporating the effects of impurities and defects have explained conduction in various materials [2–5] and are extended to the cases of spatially non-uniform trap distributions [6–8].

In experiments, we often encounter the current–voltage (*JV*) characteristics *asymmetric* with respect to the bias polarity, which exhibits the $J \propto V^m$ characteristics for *both* positive and negative polarity (J: current, V: applied voltage, $1 \leq m \leq 2$) (Fig. 1 [9]). At low voltage, the *JV* characteristics of these samples are symmetric and ohmic at both polarities (inset of Fig. 1(a)).

On the other hand, the conventional theories explain *asymmetric JV* characteristics as surface-limited conduction but cannot explain these $J \propto V^m$ characteristics (One might think that a degraded Schottky barrier can, but not when rigorously analyzed). The bulk conduction, e.g., the standard SCL conduction cannot explain these characteristics either, because it exhibits $J \propto V^2$ characteristic and is symmetric with respect to the bias polarity. It would be obvious that ohmic conduction cannot explain them, even when the spatially asymmetric distribution of the impurities or traps is included.

Although a few pioneering works [8] have shown the possibilities that the SCL conduction under some spatial distributions of traps can exhibit asymmetric *JV* characteristics, the existing theories cannot explain the experimental aspects described above. Indeed, the comparison of theory with experiments for this case is difficult to find in literature. Therefore, we have reformulated the SCL theory under a graded distribution of shallow-traps by incorporating the carrier statics rigorously.

* Tel.: +81 92 642 2538; fax: +81 92 642 2553.
E-mail address: watanabe@phys.kyushu-u.ac.jp.

0272-8842/$36.00
doi:10.1016/j.ceramint.2011.05.037

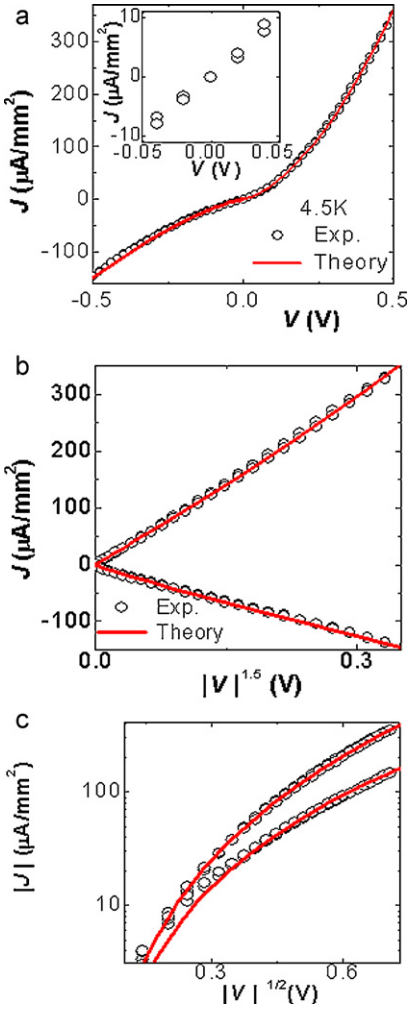

Fig. 1. Experimental *JV* characteristics of Au/$SrTiO_3$:Cr single crystal/Au (open circles) [11] and theoretical *JV* characteristics (solid lines) by the present theory for case 1 ($N_{A,k} \ll N_{t,k}$) with Eq. (18), $N_{t,k\max}/N_{t,1} = 100$, $V_{bi2} = 1.2$ mV and $J_{bi2} = 0.82$ μA mm^{-2} in (a) linear, (b) J–$V^{1.5}$ and (c) Schottky plots. Inset of 1(a) is an expanded view of the low voltage range of the main figure.

The present theory explains the above experimental aspects and reproduces exactly experimental diode-like *JV* characteristics with $J \propto V^m$ by one parameter additional to those of the standard SCL theory. That is, *the rectifying JV characteristics in* Fig. 1 a*re not of degraded Schottky barriers* (Fig. 1(c)) *but of bulk limited conduction*. As for the application of the present theory, the theory provides a basis for the identification of the location limiting conduction, which is essential for the investigations of nonvolatile reversible *R*-switching. It is worth remarking that present theory can also be implemented in frequently discussed filamentary conduction path models as seen from the formulation in Section 2.

Although *R*-switching is usually attributed to the surface due to the polarity dependence [10], its mechanism remains unresolved [11–14]. The trap density gradient assumed in the present paper is naturally expected in *R*-switching materials due to their forming process. The forming process is the creation of the traps in the originally high-resistance materials by current injection. That is, the electron impacts ionize or distort the atoms, or ions and defects may migrate. The electron impacts are expected to be proportional to the electron density, which is inversely proportional to the distance from an injecting electrode. This is because the material is initially almost insulating and the conduction obeys the standard SCL theory. Similarly, the migration of ions and defects is expected to decrease with the distance from an injecting electrode. For clarity, the present paper introduces the rectification due to graded distribution of *shallow traps* in an elementary manner.

2. Theory

We formulate a one-dimensional steady-state SCL conduction under the following assumptions commonly used in SCL conduction theories [1,2].

(1) Applied field E is not so high that the electron mobility is independent of E, and microscopic elementary processes, such as electron capture, are unchanged;
(2) Thermal energy is far lower than electrostatic energy, and thus, the diffusion current can be neglected:

$$J = qn\mu E \tag{1}$$

(q: elementary charge, n: free carrier density, μ: mobility);
(3) Current carriers are electrons (unipolar); and
(4) In-gap states near the contact are abundant so that effect of the potential barrier can be neglected and the contacts can be regarded as injecting/ohmic contacts. In addition, traps are assumed not fully filled.

We consider a one-dimensional chain of $k_{\max}$ segments with each length $L/k_{\max}$ and the total length L. Quasi-equilibrium carrier densities in the kth segment are given by the formulae:

$$n_{0,k}(x) = N_C \exp\left[\frac{-(E_{C0,k} - E_F)}{k_B T}\right] \tag{2}$$

$$n_{t0,k}(x) = \frac{N_{t,k}}{1 + g^{-1}\exp[(E_{t0,k} - E_F)/k_B T]} \tag{3}$$

$$n_k(x) = N_C \exp\left[\frac{-(E_{C,k}(x) - E_{Fn})}{k_B T}\right], \text{ and} \tag{4}$$

$$n_{t,k}(x) = \frac{N_{t,k}}{1 + g^{-1}\exp[(E_{t,k}(x) - E_{Fn})/k_B T]}. \tag{5}$$

Here, $n_{0,k}(x)$ and $n_k(x)$ are free carrier densities in the absence and presence of an external field, respectively. $n_{t0,k}(x)$ and $n_{t,k}(x)$ are carrier densities at shallow-traps defined similarly. N_C, $E_{C0,k}$, $E_{C,k}(x)$, $N_{t,k}$, g, $E_{t0,k}$, and $E_{t,k}(x)$ are the effective density states of the conduction band, the energy levels of the bottom edge of the conduction band in the absence and presence of an external field, the concentration of shallow-traps (This implies that $N_{t,k}$ is the density of donor like traps), the degeneracy factor, and the energy levels of shallow-traps in the absence and presence of an external field ($E_{t0,k} - E_F > k_B T$, $E_{t,k} - E_F > k_B T$), respectively. $E_{C,k} - E_{t,k}$ is constant. E_F, E_{Fn},

k_B, and T are the Fermi level, quasi-Fermi level, Boltzmann constant, and temperature, respectively. In addition to the shallow-traps, deep-traps having an energy level of $E_{A,k} < E_F$ with density $N_{A,k}$ are introduced and are assumed to be fully occupied and negatively charged (This means $N^-_{A,k} = N_{A,k}$). Under this assumption, the density of ionized shallow-traps in the absence of the external field $N^+_{t0,k}$ is related to $N_{t,k}$ and $n_{t0,k}$ via $N^+_{t0,k} + n_{t0,k} = N_{t,k}$.

For $N_{A,k} \ll N^+_{t0,k}$ ($\approx N_{t,k}$), the local charge neutrality $n_{0,k} = N^+_{t0,k}$ is satisfied when diffusion is weak in comparison with local macroscopic electrostatic force and an external field is absent. Consequently, we obtain

$$N^+_{t0,k} = \frac{N_{t,k}}{1 + g\exp[-(E_{t0,k} - E_F)/k_BT]} = n_{0,k}. \tag{6}$$

Because Eq.(6) suggests that $n_{0,k}$ increases with $N_{t,k}$, $E_{C0,k}$ shifts gradually with k when $N_{t,k}$ changes with k. Therefore, we may estimate the upper limit of a built-in potential in this system, i.e., a diffusion potential (ΔE_{C0})

$$\Delta E_{C0} = E_{C0,k\max} - E_{C0,1} \fallingdotseq k_BT \ln\left(\frac{N_{t,k\max}}{N_{t,1}}\right) \tag{7}$$

ΔE_{C0} is approx. 40 meV at room temperature (RT) for $N_{t,k\ \max}/N_{t,1} = 5$.

We consider two cases of electron distributions. The case for increasing $n_{0,k}$ with $N_{t,k}$ is already examined in the preceding paragraph (case 1). As the case 2, we examine $N_{A,k} \fallingdotseq N^+_{t0,k}$. In this case, the local charge neutrality $n_{0,k} = N^+_{t0,k} - N_{A,k}$ leads to $n_{0,k} \ll N^+_{t0,k} \fallingdotseq N_{A,k}$, because the most carriers in deep-traps are trapped. In case 2, $n_{0,k}$ can be approximated to be independent of $N^+_{t0,k}$, and its variation in Poisson's equation is unimportant. Therefore, as an alternate representative case, we study the case 2 where $n_{0,k}$ is constant ($n_{0,k} = n_0$), implying that $E_{C0,k}$ is constant ($E_{C0,k} = E_{C0}$). This leads to

$$E_{C,k}(x) = E_{C0} - qV(x). \tag{8}$$

The case $N_{A,k} \gg N^+_{t0,k}$ is not included in the cases 1 and 2 of electron distributions discussed here. This case can be regarded as the deep trap case and is discussed in refs. [15,16], which report a rigorous formulation for general trap distributions.

We derive equations for the above two electron-distributions (cases 1 and 2). Local charge neutrality is approximately satisfied in the absence of an external field. Therefore, the net charge density under an external field for $qV \gg \Delta E_C$ is a net increase of the sum of the free and trapped charge densities; for $E_{t,k}(x) - E_{Fn} > k_BT$ and $E_{t0,k} - E_F > k_BT$, we obtain

$$\frac{\varepsilon dE(x)}{dx} = -q(n(x) - n_{0,k})\,(1 + \Theta_k^{-1}) \tag{9}$$

where $\Theta_k \equiv n(x)/n_{t,k}(x)$. In this derivation, we used the relationship

$$\Theta_k \fallingdotseq N_C \exp\frac{\left[(E_{t0,k} - E_{C0,k})/k_BT\right]}{gN_{t,k}} = \frac{n_{0,k}}{n_{t0,k}}. \tag{10}$$

The solution is given in terms of dimensionless quantities

$$u \equiv \frac{N_*}{n(x)}, \quad W \equiv \frac{L}{L_*} \tag{11}$$

$$W_k \equiv \frac{L}{k_{\max}L_*}, \quad v = \frac{|V|}{V_{\text{bi2}}}, \quad \text{and} \tag{12}$$

$$\eta_k = \frac{N_{t,k}}{N_*} \tag{13}$$

where

$$\frac{1}{L_*} \equiv \frac{N_*^2q^2\mu(1 + \Theta_1^{-1})}{\varepsilon|J|}, \tag{14}$$

$$V_{\text{bi2}} \equiv \frac{N^*qL^2(1 + \Theta_1^{-1})}{\varepsilon}. \tag{15}$$

Here, L_* and N_* are typical values of L and $N_{t,k}$, respectively, and Θ_1 is $\Theta_{k=1}$ for $N_{t,1} \equiv N_{t,k\ =1}$.

The boundary conditions are $E(0) = V(0) = 0$ (or $E(L) = V(L) = 0$) and the continuity of $E(x)$ and $V(x)$ at x_k.

The solution is given by the recurrence formulae (case 1)

$$\begin{aligned} v(x_k)\ &- v(x_k - 1) \\ &= \frac{1}{\theta_k}\left[-\frac{u_k^2 - u_{k-1}^2}{2\eta_k} - \frac{u_k - u_{k-1}}{\eta_k^2}\right. \\ &\quad \left. - \frac{\ln\left(|1 - \eta_k u_k|/|1 - \eta_k u_{k-1}|\right)}{\eta_k^3}\right] \end{aligned} \tag{16}$$

$$-\frac{u_k - u_{k-1}}{\eta_k} - \frac{\ln\left(|1 - \eta_k u_k|/|1 - \eta_k u_{k-1}|\right)}{\eta_k^2} = \theta_k W_k \tag{17}$$

where $u_k \equiv u(x_k)$ and $\theta_k = (1 + \Theta_k^{-1})/(1 + \Theta_1^{-1})$.

Here, we postulate that shallow-traps are not full also during injection. The free parameters are $n_{0,k} = N^+_{t,k}$, η_k, θ_k, and W_k, where $\theta_k = (\Theta_1 + \Theta_1/\Theta_k)/(\Theta_1 + 1)$. Using above relationships, we obtain $\Theta_\kappa/\Theta_1 = N_{t,1}/N_{t,k}{=}\eta_1/\eta_k$, $\theta_k = (\Theta_1 + \eta_k/\eta_1)/(\Theta_1 + 1)$, and $N^+_{t,1}/N^+_{t,k} \approx N_{t,1}/N_{t,1}.$, where we used the relationship that $N_{t0}{}^+{}_{,k}$ is approximately proportional to $N_{t,k}$ owing to Eq.(6). Therefore, free parameters in Eqs. (16) and (17) are η_k and Θ_1.

For $N_{A,k} \fallingdotseq N_{t,k}$ (case 2), we obtain the solution by setting $\eta_k = 1$ for all k in Eqs. (16) and (17) but keeping the relationship $\theta_k = (\Theta_* + N_{t,k}/N_{t,1})/(\Theta_* + 1)$ for θ_k. Therefore, the free parameters are $N_{t,k}/N_{t,1}$ (k = 1-$k_{\max}$), Θ_* and n_0.

JV characteristics can be calculated for given distributions of $N_{t,k}$. By setting the boundary values $N_{t,1}/N_*$ and $N_{t,k\max}/N_*$, we consider exponential

$$N_{t,k} \propto \exp(-bx) \tag{18}$$

and linear distributions

$$N_{t,k} \propto 1 - \frac{x}{L} \tag{19}$$

where b is a constant.

Numerical *JV* characteristics are shown in normalized form by

$$v = \frac{|V|}{V_{\mathrm{bi2}}} \text{ and} \tag{20}$$

$$j = \frac{|J|}{J_{\mathrm{bi2}}} \tag{21}$$

where

V_{bi2} is twice the built-in potential of the system, and

$$J_{\mathrm{bi2}} = \frac{N_* q \mu V_{\mathrm{bi2}}}{L} \tag{22}$$

is an ohmic current due to V_{bi2}.

Typical values are estimated for $\Theta_1 = 1$:

$$V_{\mathrm{bi2}} = \frac{18(N_*/10^{16}\ \mathrm{cm^{-3}})(L/10^{-5}\,\mathrm{cm})^2}{\varepsilon/(200 \times 8.9 \times 10^{-14}\ \mathrm{F\ cm^{-1}})}[\mathrm{mV}] \tag{23}$$

and

$$J_{bi2} = \frac{46(N_*/10^{16}\ \mathrm{cm^{-3}})\,(\mu/10^{-3}\ \mathrm{cm^2\ V^{-1}\ s^{-1}})}{L/10^{-5}\,\mathrm{cm}} \times (V_{\mathrm{bi2}}/18\,\mathrm{mV}) \times [\mu\mathrm{A\ mm^{-2}}]. \tag{24}$$

In these estimations, L should be regarded as the length of the region where the shallow-trap density changes exponentially or linearly. This is because the *JV* characteristics are dominated by high resistance regions, i.e., low trap density regions; thus, the details of the low resistance regions are unimportant. In addition, we can use the following results for hole conduction, by, for instance, regarding the case $1(N_{A,k} \ll N_{t,k})$ as the case $N_{D,k} \ll N_{t,k}$ ($N_{D,k}$: donor density).

3. Comparison with experiments

In Fig. 2, theoretical *JV* characteristics for forward and reverse bias are plotted for cases 1 and 2 ($N_{A,k} \ll N_{t,k}$ and $N_{\mathrm{A},k} \fallingdotseq N_{t,k}$) with linear distributions. At low voltage ($v \ll 1$), the *JV* characteristics follow Ohm's law, and at high voltage ($v \gg 1$), they follow the standard Mott–Gurney law ($J \propto V^2$). Fig. 2 demonstrates that the conductance at low voltage is symmetric, i.e., same for forward and reverse bias. At high voltage, however, the current density is higher under forward bias than under reverse bias. For case 2 ($N_{\mathrm{A},k} \fallingdotseq N_{t,k}$) (Fig. 2(b)), the ohmic conductance at low voltage are the same for $N_{t,k\mathrm{max}}/N_{t,1} = 100$ and $N_{t,k\mathrm{max}}/N_{t,1} = 10$, because n_0 is the same in both cases. The results for exponential distributions are similar to those of linear distributions except for the larger conductance difference between the forward and the reverse bias. Fig. 3 shows that m changes more gradually for case 1 ($N_{\mathrm{A},k} \ll N_{t,k}$) than for case 2 ($N_{\mathrm{A},k} \fallingdotseq N_{t,k}$).

The present theory for case 1 ($N_{\mathrm{A},k} \ll N_{t,k}$) reproduces experimental *JV* curves excellently by choosing $N_{t,k\mathrm{max}}/N_{t,1}$ and scaling the theoretical curve at one data point from either a forward or a reverse branch of *JV* curve (Figs. 1 and 4). Because theoretical *JV* curves are insensitive to Θ_1, we fix Θ_1 at 0.01. Consequently, $N_{t,k\mathrm{max}}/N_{t,1}$, V_{bi2} and J_{bi2} are only free

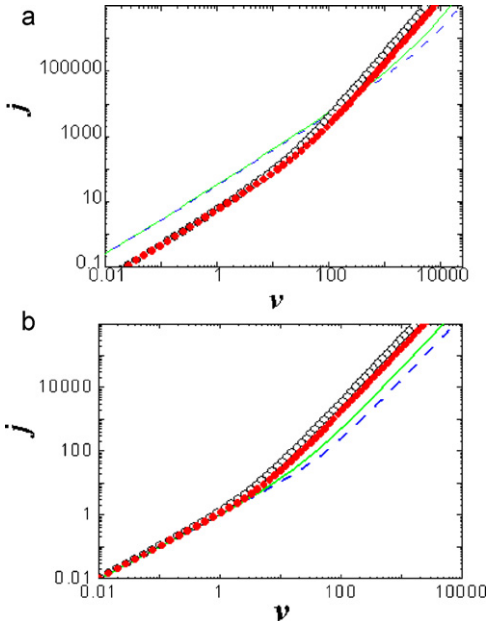

Fig. 2. Theoretical *JV* characteristics for (a) case $1(N_{A,k} \ll N_{t,k})$ and (b) case 2 ($N_{A,k} \cong N_{t,k}$) with linear distributions (Eq. (19)) and $\Theta_0 = 0.01$: open and filled circles are the forward bias and the reverse bias branch of the solution for $N_{t,k\mathrm{max}}/N_{t,1} = 10$, respectively, and solid and dashed lines are the forward bias and the reverse bias branch of the solution for $N_{t,k\mathrm{max}}/N_{t,1} = 100$, respectively. j and v are a normalized absolute current density and a normalized absolute voltage. One would see $j \propto v$ at low voltages and $j \propto v^2$ at high voltage.

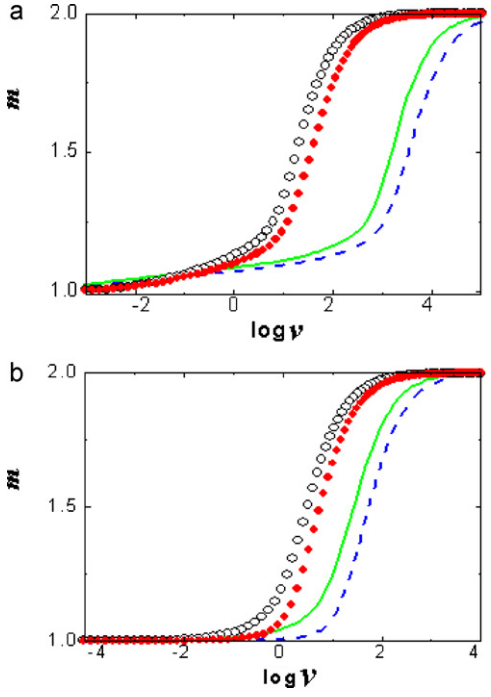

Fig. 3. Theoretical exponent m vs. normalized voltage (v) for (a) case 1 ($N_{A,k} \ll N_{t,k}$) and (b) case 2 ($N_{A,k} \cong N_{t,k}$) with linear distributions (Eq. (19)) derived from Fig. 2: open and filled circles are for $N_{t,k\mathrm{max}}/N_{t,1} = 10$ at forward and reverse bias, and solid and dashed lines are for $N_{t,k\mathrm{max}}/N_{t,1} = 100$ at forward and reverse bias, respectively.

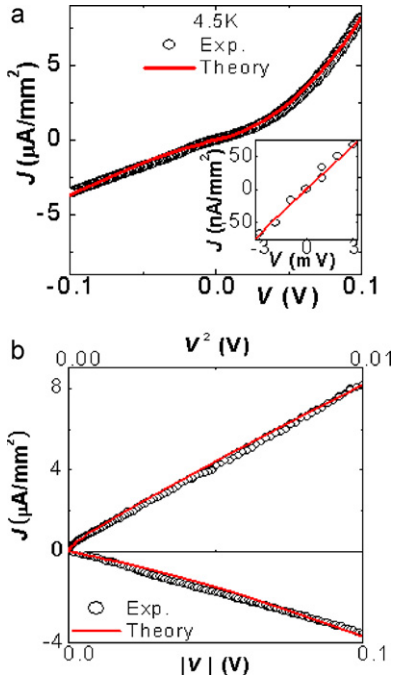

Fig. 4. Experimental *JV* characteristics (open circles) of Au/$SrTiO_3$:Cr single crystal/Au [9] and theoretical *JV* characteristics by present theory (solid lines)(a). (b) *JV* characteristics for forward and reverse bias in a linear plot (a) are replotted in a J–V^2 ($V \geq 0$) and a linear plot ($V \leq 0$). The fitting parameters are $N_{t,k\max}/N_{t,1} = 1000$, $V_{bi2} = 110$ mV and $J_{bi2} = 0.23$ μA mm^{-2} in $N_{A,k} \cong N_{t,k}$. The inset of (a) is an expanded view of the low voltage range of the main figure.

parameters in practice. N_* and L obtained from V_{bi2} and J_{bi2}, especially those of Fig. 2, compare favorably with experimental values. In Fig. 1(c), the lack of linearity in the Schottky plots contrasts with the excellent linearity of the J–V^m plots. This provides further support for the concept that the observed diode properties are not due to surface-limited processes.

4. Conclusions

The present paper has presented an introduction for bulk-originated rectification with nonrigorous formulation and shown diode-like *JV* characteristics due to a bulk-limited conduction process. We have shown that a symmetric ohmic conduction appears at low voltage but diode-like *JV* characteristics with the $J \propto V^m$ ($m = 1$–2) appear at high voltage. The present theory reproduces experimental data excellently using three free parameters $N_{t,k\max}/N_{t,1}$, V_{bi2}, and J_{bi2}—one parameter more than in the standard SCL conduction theory. Rigorous formulation for general cases including deep-trap dominated case and detailed discussions are presented in Refs. [15,16]. Ref. [16] shows that Eqs. (16) and (17) with $k_{\max} = 2$ can fit sufficiently data, which greatly facilitate the use of the present theory.

Acknowledgement

The author acknowledges the permission of the use of unpublished data to Dr. J. G. Bednorz, useful discussions to him and Dr. Alvarado, and La Mattina.

References

[1] N.F. Mott, R.W. Gurney, Electronic Processes in Ionic Crystals, Oxford University Press, London, 1948.
[2] J.P. Ibbetson, U.K. Mishra, Space-charge-limited currents in nonstoichiometric GaAs, Applied Physics Letters 68 (1996) 3781–3783.
[3] H. Okushi, Carrier transport on p^+–ν junction based on relaxation semiconductors. I. theory, Japanese Journal of Applied Physics 18 (1979) 779–789.
[4] Y. Kim, S. Ohmi, K. Tsutsui, H. Iwai, Space-charge-limited currents in La_2O_3 thin films deposited by E-beam evaporation after low temperature dry-nitrogen annealing, Japanese Journal of Applied Physics 44 (2005) 4032–4042.
[5] G.T. Wright, Solid State Electronics 2 (1961) 165–189.
[6] N. Koda, Space-charge-limited currents in insulators with nonuniform spatial distribution of shallow traps, Japanese Journal of Applied Physics 25 (1986) 200–204.
[7] M.-A. Nicolet, Unipolar space-charge-limited current in solids with nonuniform spatial distribution of shallow traps, Journal of Applied Physics 37 (1966) 4224–4235.
[8] J. Sworakowski, Space-charge-limited currents in solids with nonuniform spatial trap distribution, Journal of Applied Physics 41 (1970) 292–295.
[9] Y. Watanabe, J.G. Bednorz, unpublished results.
[10] A. Baikalov, Y.Q. Wang, B. Shen, B. Lorenz, S. Tsui, Y.Y. Sun, Y.Y. Xue, Applied Physics Letters 83 (2003) 957–959.
[11] Y. Watanabe, Electrical transport through Pb(Zr,Ti)O_3 *p–n* and *p–p* heterostructures modulated by bound charges at a ferroelectric surface: ferroelectric *p–n* diode, Physical Review B 59 (1999) 11257–11266.
[12] Y. Watanabe, D. Sawamura, M. Okano, Recurrent local resistance breakdown of an epitaxial $BaTiO_3$/$SrTiO_3$ heterostructure, Applied Physics Letters 72 (1998) 2415–12415.
[13] Y. Watanabe, J.G. Bednorz, A. Bietsch, Ch. Gerber, D. Widmer, A. Beck, S.J. Wind, Current-driven insulator-conductor transition and nonvolatile memory in chromium-doped $SrTiO_3$ single crystals, Applied Physics Letters 78 (2001) 3738–3740.
[14] S.F. Alvarado, F. La Mattina, J.G. Bednorz, Electroluminescence in $SrTiO_3$:Cr single-crystal nonvolatile memory cells, Applied Physics A 89 (2007) 85–89.
[15] Y. Watanabe, Unidirectional current flow due to nonlinear bulk conduction under trap density gradient, Journal of the Physical Society of Japan 78 (2009) (104712-1–104712-10).
[16] Y. Watanabe, Unidirectional bulk conduction and the anomalous temperature dependence of drift current under a trap-density gradient, Physical Review B 81 (2010) (195210-1–195210-14).